Synergistic catalysis for light-driven proton reduction using a polyoxometalate-based Cu-Ni heterometallic–organic framework

Wenlong Sun,[a] *Cheng He,*[a] *Tao Liu,*[a] *and Chunying Duan**[a,b]

[a]Chemical School of Zhang Dayu State Key Laboratory of Fine Chemicals; Dalian University of Technology; Dalian 116024, China

[b]Collaborative Innovation Center of Chemical Science and Engineering; Tianjin 300071, China

Corresponding Authors

*E-mail: cyduan@dlut.edu.cn.

Table of contents

1. General Methods and Materials.

All solvents and chemical materials for syntheses were purchased from commercial sources and used as received without further purification. Mass Spectra were recorded on a GC-MS (Agilent 7890B/5977B) instrument in EI mode. The elemental analyses were of C, H and N conducted on a Vario EL III elemental analyzer, and that of W, P, Cu and Ni were analyzed on a Jarrel-AshJ-A1100 (ICP) atomic emission spectrometer. The X-ray powder diffraction (XRPD) patterns were recorded with a Bruker AXS D8 Advance diffractometer instrument with Cu *K*α radiation (λ=1.54056 Å) in the angular range 2θ = 5–50° at 293K. Thermogravimetric analysis (TGA) was carried out at a ramp rate of 10°C/min in a nitrogen flow with a Mettler-Toledo TGA/SDTA851 instrument. The generated photoproduct of H_2 was characterized by GC-7890T instrument analysis using a 5Å molecular sieve column (0.6m×3mm), thermal conductivity detector, and nitrogen used as carrier gas. The samples were irradiated by a 300 W Xenon Lamp (CEL-HXUV300). W element valence were analyzed on a XPS spectra. IR spectra were recorded as KBr pellets on a NEXUS instrument. Solid UV-vis spectra were recorded on a U-4100 spectrometer. Liquid UV-vis spectra were performed on a TU-1900 spectrophotometer. Solid fluorescent spectra were measured on a JASCO FP-6500 instrument. ZAHNER ENNIUM electrochemical workstation was used for control of the electrochemical measurements and data collection. A conventional three-electrode system was used, with a modified carbon paste electrode (CPE) or glassy carbon electrode as a working electrode, a twisted platinum wire as counter electrode, and a commercial Ag/AgCl as

a reference electrode. ^{1}HNMR was measured on a Varian INOVA-400/500 spectrometer with chemical shifts reported as ppm (in DMSO-d_6 or $CDCl_3$). Analysis of yield in the organic reaction was performed using Agilent 7820A gas-chromatography system equipped with a thermosconductivity detector with N_2 as a carrier gas. Scanning electron microscopy (SEM) images were taken with a NOVA NanoSEM 450 microscope. All confocal laser scanning microscopy (CLSM) micrographs were collected by Olympus Fluoview FV1000. Products were purified by flash column chromatography on 200–300 mesh silica gel SiO_2.

2. Experimental Section.

Synthesis of 4,4'-(1,4-phenylene) bis-Pyridine (PBPY) was prepared according to the literature methods[S1] and characterized by ^{1}HNMR. (400 MHz, $CDCl_3$): δ= 8.71 (d, *J* = 6.0 Hz, 4H), 7.77 (s, 4H), 7.56 (d, *J* = 6.0 Hz, 4H).

Synthesis of Cu-Ni-POM: A mixture of $K_6[P_2W_{18}O_{62}]\cdot 14H_2O$ (90mg, 0.02mmol), PBPY (10 mg, 0.05mmol), $Cu(NO_3)_2\cdot 3H_2O$ (24 mg, 0.1mmol), $Ni(NO_3)_2\cdot 6H_2O$ (29 mg, 0.1mmol), and oxalic acid (OX) (25 mg, 0.28mmol) were dissolved in 8mL solvents of H_2O in ascrew-capped vial. The pH of the mixture was adjusted to about 3.1 with 1.0 mol/L NaOH, the suspension was put into a Teflon-lined autoclave and kept under autogenous pressure at 160°C for 3 days. After cooling the autoclave to room temperature, green block single crystals were separated, washed with water and air-dried. Yield: 40 % (based on the crystal dried in vacuum). Elemental analyses Calcd for $C_{156}H_{120}N_{18}O_{92}P_2W_{18}Cu_{4.5}Ni_{4.5}$ (7629.75): C, 24.53; H, 1.57; N, 3.30; P, 0.81; W, 43.40; Cu, 3.77; Ni, 3.48. Found: C, 24.45; H, 1.59; N, 3.39; P, 0.85; W,

43.50; Cu, 3.71; Ni, 3.35.

Table S1 Optimization of the reaction conditions[a]

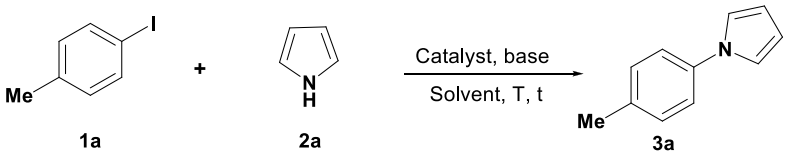

1a 2a 3a

Entry	Catalyst (mol%)	Base	Solvent	Yield (%)[b]
1	Cu-Ni-POM (0.4)	NaOH	DMSO	97
2	$Cu(NO_3)_2$ (10)	NaOH	DMSO	51
3	MOF-199 (2.5)	NaOH	DMSO	83[S2]
4	No	NaOH	DMSO	0
5	Cu-Ni-POM (0.4)	Na_2CO_3	DMSO	15
6	Cu-Ni-POM (0.4)	Cs_2CO_3	DMSO	75
7	Cu-Ni-POM (0.4)	K_3PO_4	DMSO	80
8	Cu-Ni-POM (0.4)	NaOH	DMF	10
9	Cu-Ni-POM (0.4)	NaOH	DMAC	51
10	Cu-Ni-POM (0.4)	NaOH	Dioxane	67
11	Cu-Ni-POM (0.4)	NaOH	DMSO	42[c]
12	Cu-Ni-POM (0.4)	NaOH	DMSO	87[d]
13	Cu-Ni-POM (0.4)	NaOH	DMSO	48[e]
14	Cu-Ni-POM (0.4)	NaOH	DMSO	79[f]
15	Cu-Ni-POM (0.4)	NaOH	DMSO	97[g]
16	Cu-Ni-POM (0.4)	NaOH	DMSO	96[h]

[a]Reaction conditions: 1a (0.5 mmol), 2a (1 mmol), Cu-Ni-POM catalyst (0.4 mmol% based on the molecule cage unit), base (1.0 mmol), solvent (1 mL), 120 °C, 12 h. [b]Isolated yield. [c]80°C. [d]8h. [e]NaOH (0.25 mmol). [f]NaOH (0.5 mmol). [g]2runs. [h]3runs.

Typical procedure for C-N Coupling Reaction: To a 10 mL of tube were added Cu-Ni-POM (2 umol), aryl halides (0.50 mmol), N-containing heterocycles (1 mmol),

NaOH (1.0 mmol) and DMSO (1 mL). The reaction mixture was reacted at 120 °C in a preheated oil bath for 12 h. The reaction mixture was cooled to room temperature and extracted with ethyl acetate (20 mL×3). The combined organic phases were washed with water and brine, dried over anhydrous Na_2SO_4, and concentrated in vacuo. The residue was purified by flash column chromatograph on silica gel (ethyl acetate/petroleum ether as the eluent) to afford the target products.

Table S2. Photoreductive Hydrogen Production.[a]

Catalyst (umol)	Solvent	Light (nm)	electron donor	Time (h)	TON
Cu-Ni-POM (0.1)	H_2O+acetone	200-400	MeOH	24	240
Cu-Ni-POM (0.1)	H_2O+acetonitrile	200-400	MeOH	24	trace
Cu-Ni-POM (0.1)	H_2O+C_2H_5OH	200-400	MeOH	24	trace
Cu-Ni-POM (0.1)	H_2O+DMF	200-400	MeOH	24	trace
Cu-Ni-POM (0.1)	H_2O+acetone	no	MeOH	24	no
Cu-Ni-POM (0.1)	H_2O+acetone	200-400	no	24	trace
2 Runs	H_2O+acetone	200-400	MeOH	24	230
3Runs	H_2O+acetone	200-400	MeOH	24	220

[a]reaction condition: the solution total volume of 4mL, and MeOH (25% v:v) in a H_2O/solvent (1:2 in volume) solution at 25°C resulted in the 200-400nm (UV) light irradiation.

The ICP-MS experiments analysis of the Cu-Ni-POM showed that Cu, Ni, P and W element proportion almost no loss after reaction.

Typical procedure of Photoreductive Hydrogen Production: Photoinduced hydrogen evolution was made in a 20mL flask. Varying kinds of the Cu-Ni-POM catalyst and MeOH (V, 25%) in 2:1 Me_2CO/H_2O were added to obtain a total volume of 4mL. The flask was sealed with a septum, degassed by bubbling nitrogen for 20 min under

atmospheric pressure at room temperature. After that, the samples were irradiated by a 300 W Xenon Lamp, the reaction temperature was 293 K by using a water filter to absorb heat. The generated photoproduct of H_2 was characterized by GC 7890T instrument analysis using a 5Å molecular sieve column (0.6m×3mm), thermal conductivity detector, and nitrogen used as carrier gas. The amount of hydrogen generated was determined by the external standard method. Hydrogen in the resulting solution was not measured and the slight effect of the hydrogen gas generated on the pressure of the flask was neglected for calculation of the volume of hydrogen gas.

3. Single Crystal Analyses of the Complexes.

3.1 Crystallography

Single-crystal X-ray diffraction data for Cu-Ni-POM were collected on a Bruker SMART APEX CCD diffractometer with graphite-monochromated Mo-Kα (λ = 0.71073Å) using the SMART and SAINT programs.[S3,S4] Routine Lorentz polarization and Multi-scan absorption correction were applied to intensity data. The structures were determined, and the heavy atoms were identified by direct methods using the SHELXTL-97 program package.[S5] The hydrogen atoms of PBPY ligands were generated geometrically for compound Cu-Ni-POM, while the hydrogen atoms of water molecules can not be found from the residual peaks and were directly included in the final molecular formula. The detailed crystallographic data and structure refinement parameters are summarized in Table S3. Crystallographic data for the structure reported in this paper have been deposited in the Cambridge Crystallographic Data Center with CCDC Number: 1875777.

Table S3 Crystal data and structure refinements for Cu-Ni-POM.

Compound	Cu-Ni-POM
Formula	$C_{156}H_{120}N_{18}O_{92}P_2W_{18}Cu_{4.5}Ni_{4.5}$
Formula weight	7629.75
Crystal system	trigonal
Space group	*P6/m*
a/Å	18.858(5)
b/Å	18.858(5)
c/Å	15.577(5)
α, deg	90
β, deg	90
γ, deg	120
V/Å^3	4797(2)
Z	1
D_{calcd}/g cm^{-3}	2.641
T/K	293(2)
μ/mm^{-1}	11.772
Refl. Measured	29458
Refl. Unique	3782
R_{int}	0.1201
GoF on F^2	0.988
R_1/wR_2 [$I \geq 2\sigma(I)$]	0.0641/0.1826

$R_1 = \sum \| F_o | - | F_c \| / \sum | F_o |$. $wR_2 = \sum[w(F_o^2 - F_c^2)^2] / \sum[w(F_o^2)^2]^{1/2}$

3.2 Cu-Ni-POM of Structure.

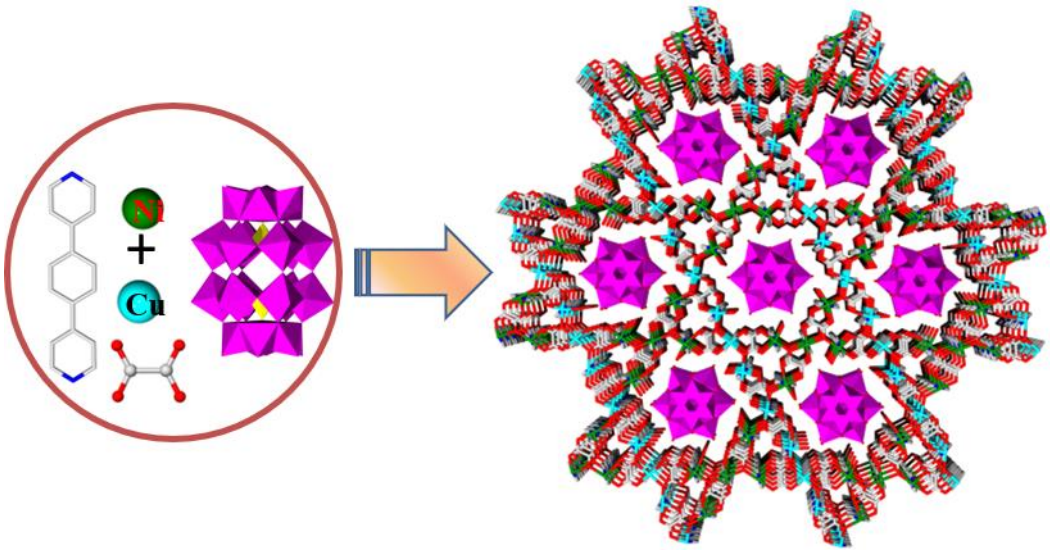

Figure S1. View of the assembly process showing constitute of the three-dimensional structures, Show of $[P_2W_{18}O_{62}]^{6-}$, OX, Ni^{II}, Cu^{II} and PBPY fragment.

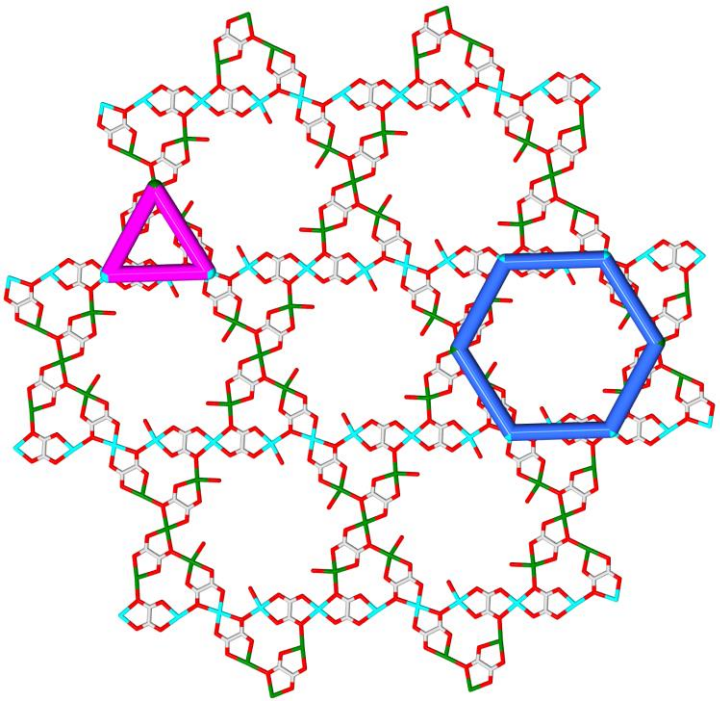

Figure S2. View of 2D metal organic layer with triangular and hexagonal structures.

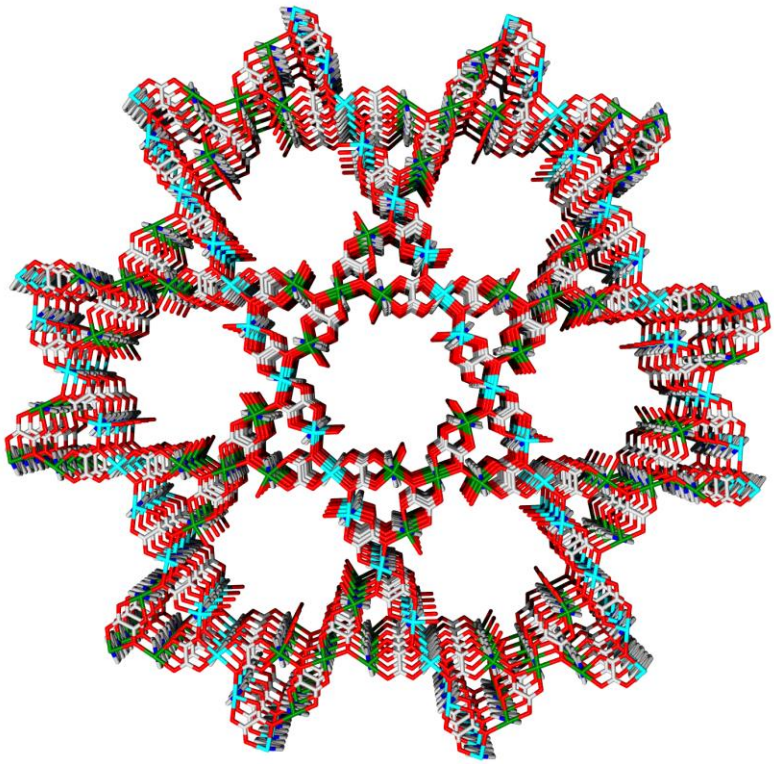

Figure S3. Face view of the three-dimensional Metal Organic Framework structure along the b axis direction.

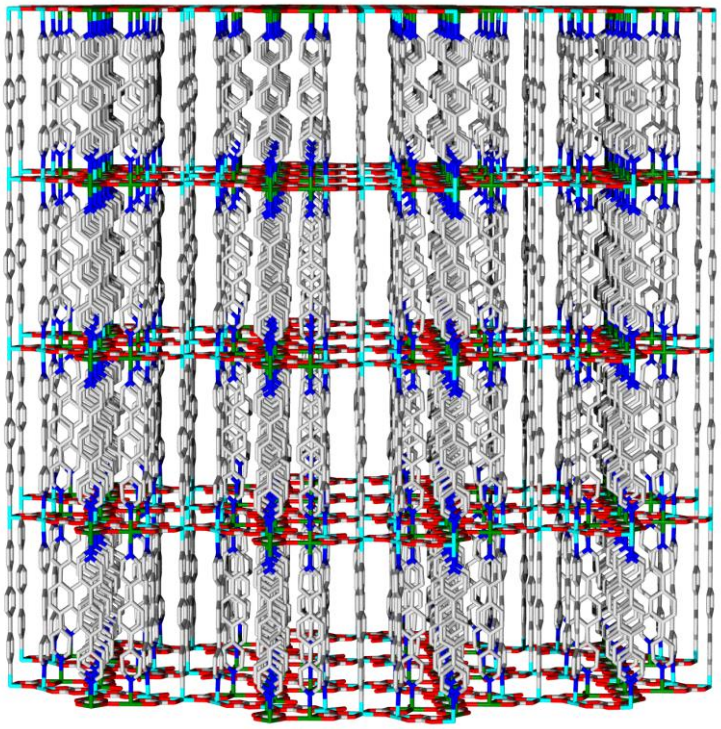

Figure S4. View of the three-dimensional Metal Organic Framework along the c axis direction.

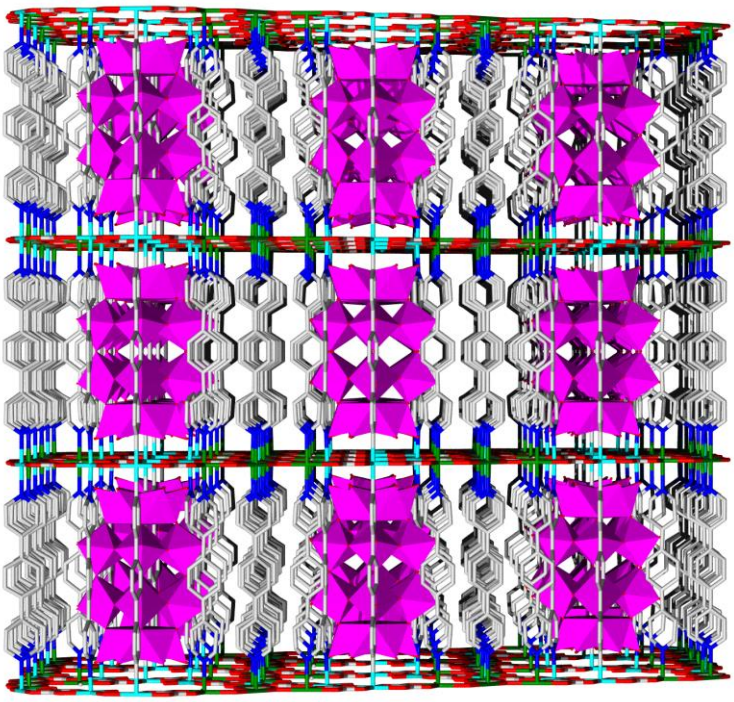

Figure S5. View of the three-dimensional structure, showing the embedded $[P_2W_{18}O_{62}]^{6-}$ units within the pores along the c axis direction.

4. Confocal images.

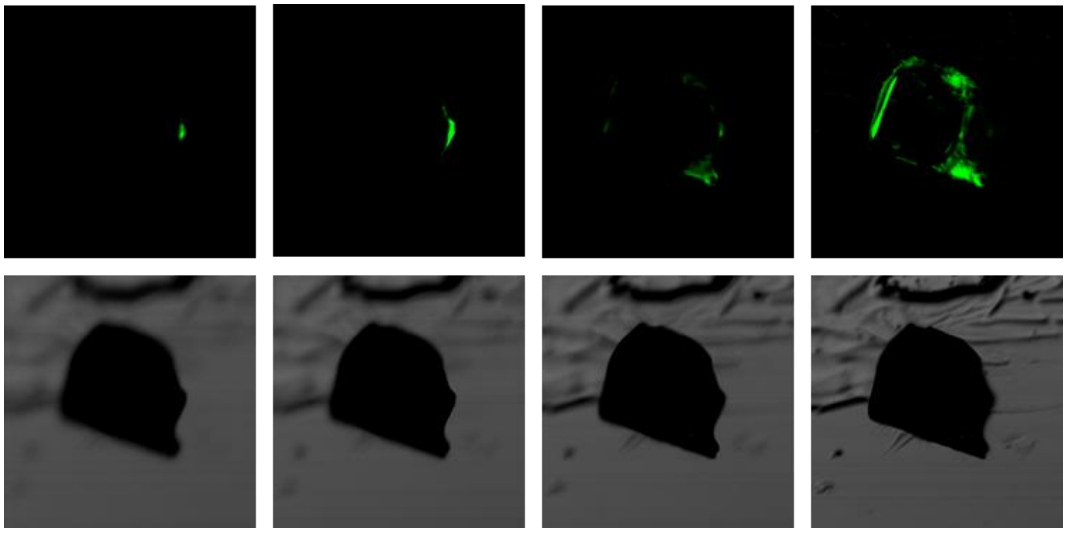

Figure S6. Confocal images of soaked fluorescence in dye of Cu-Ni-POM.

5. Crystal of Characteristics.

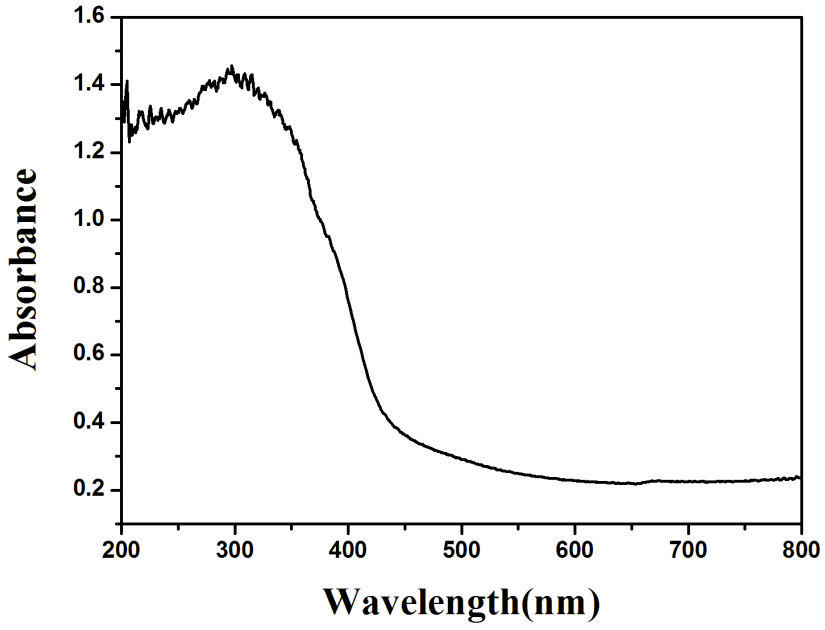

Figure S7. Solid state UV-Vis absorption spectra of Zn-POM.

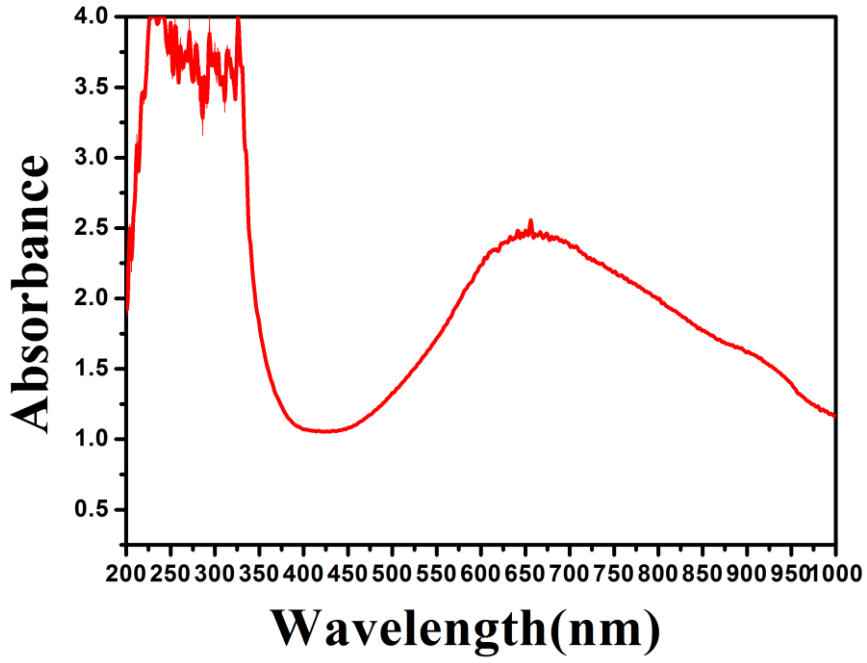

Figure S8. Solution state UV-Vis absorption spectra of Zn-POM suspension (HPB) after irradiation.

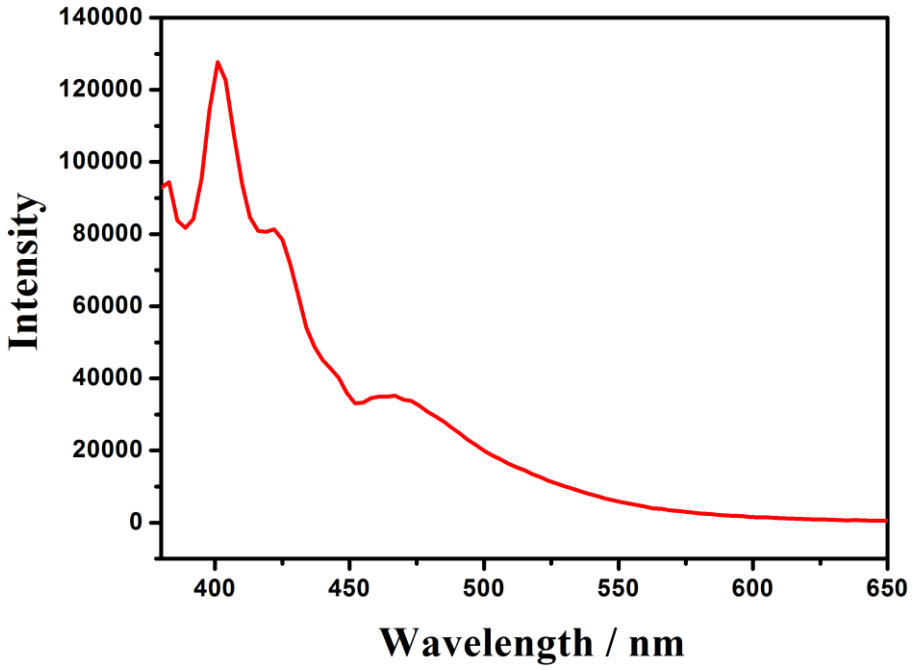

Figure S9. Solid state emission spectra of Cu-Ni-POM in MeCN suspension solution.

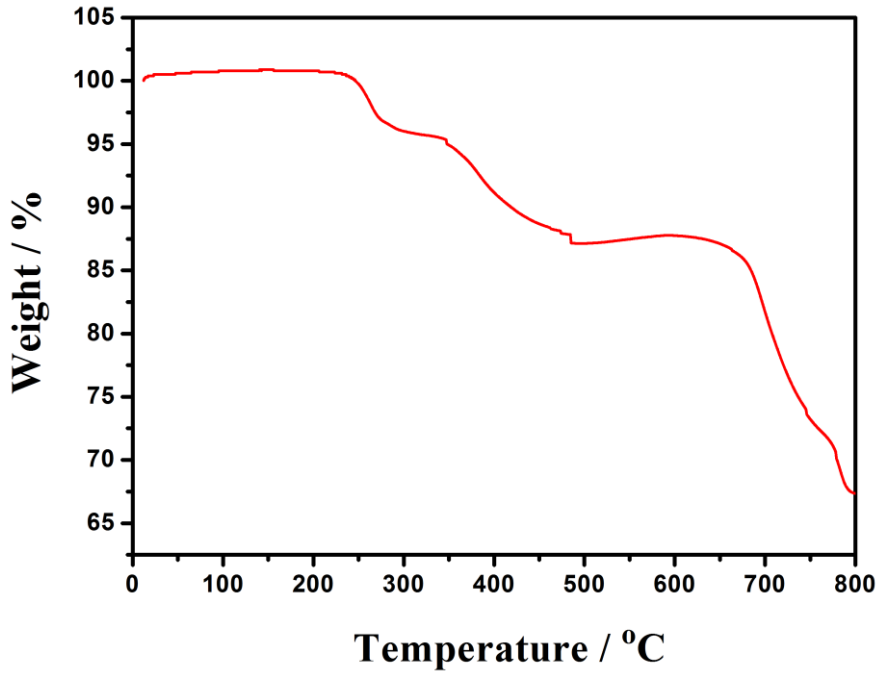

Figure S10. TG curves of Cu-Ni-POM in the flowing N_2 atmosphere.

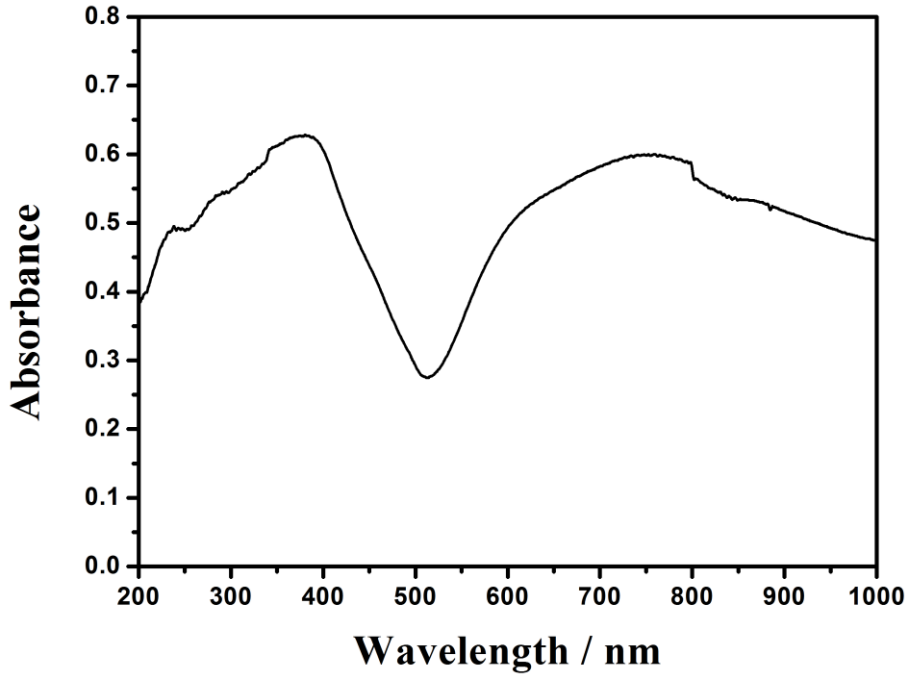

Figure S11. Solid state UV-Vis absorption spectra of Cu-Ni-POM.

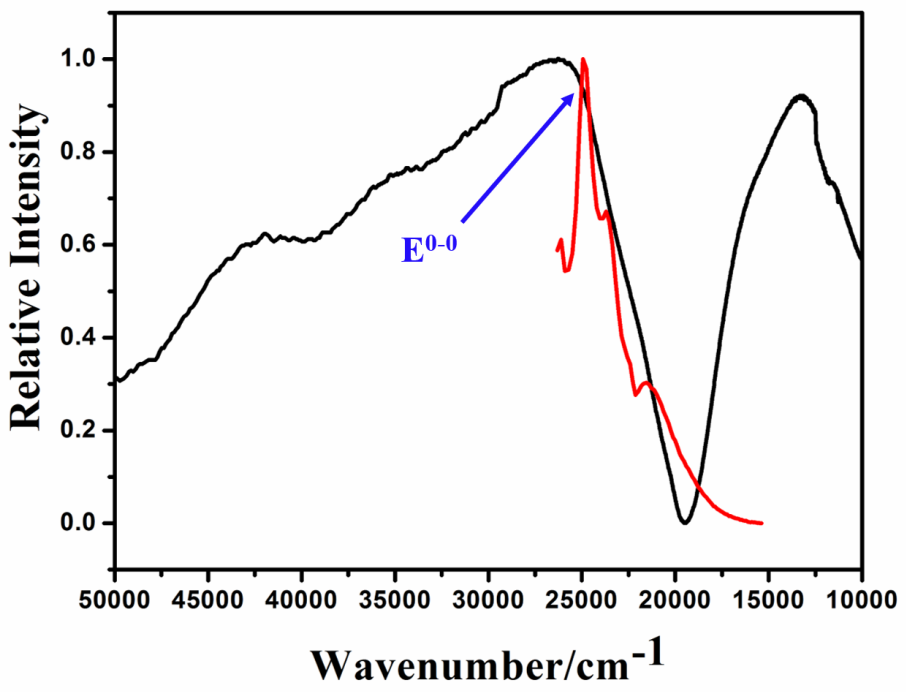

Figure S12. Normalized absorption (black line) and emission spectra (red line) of Cu-Ni-POM, excited at 350 nm.

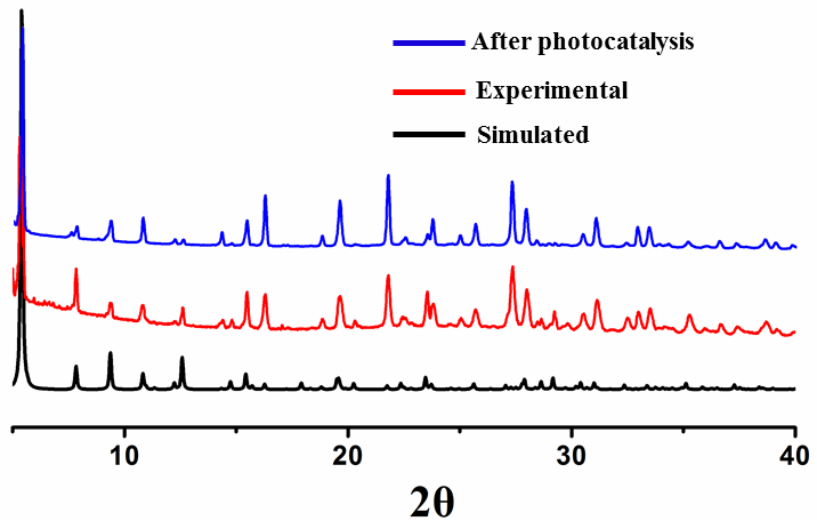

Figure S13. PXRD patterns of Cu-Ni-POM**:** its calculated pattern based on the single-crystal simulation (black), the experimental synthesis (red), and the catalyst after reactions (blue).

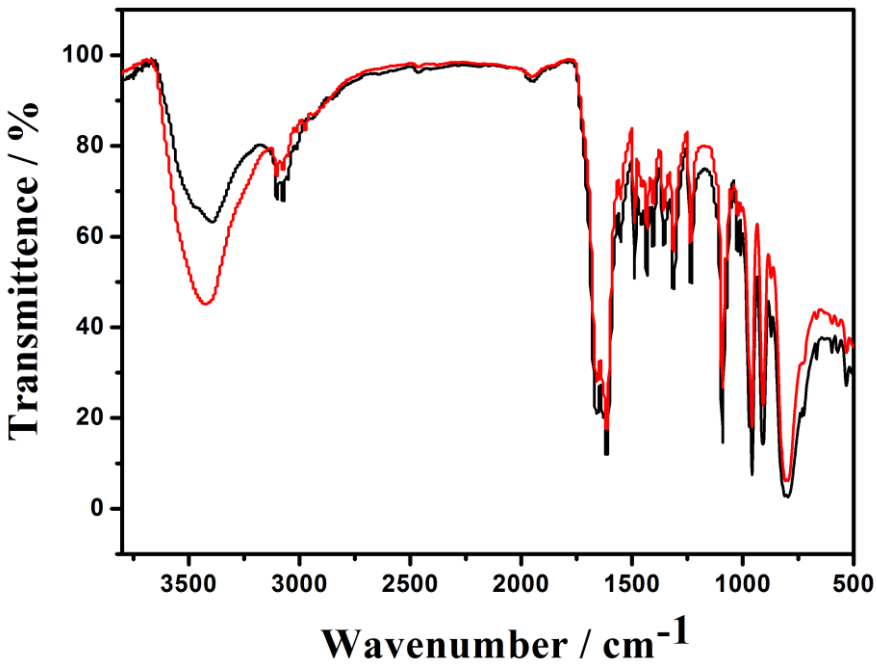

Figure S14. IR spectra of Cu-Ni-POM: the experimental synthesis (black) and the catalyst after reactions (red).

6. Cu-Ni-POM of Optical image

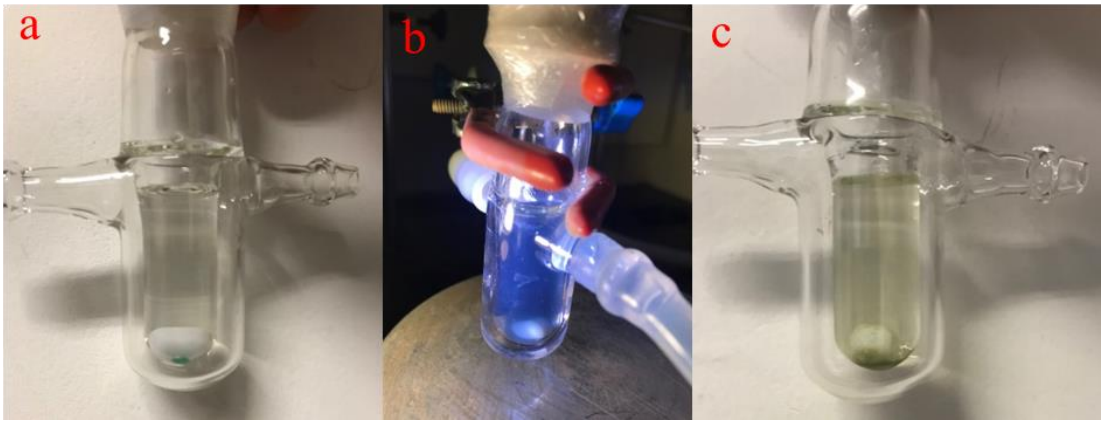

Figure S15. Optical image: heteropolyacid (HPA) of Cu-Ni-POM suspension solution before irradiation (a), heteropoly blue (HPB) of Cu-Ni-POM suspension solution after irradiation (b), HPB turn to HPA of Cu-Ni-POM suspension solution after expose air or O_2 atmosphere (c).

7. SEM image of the Cu-Ni-POM crystal.

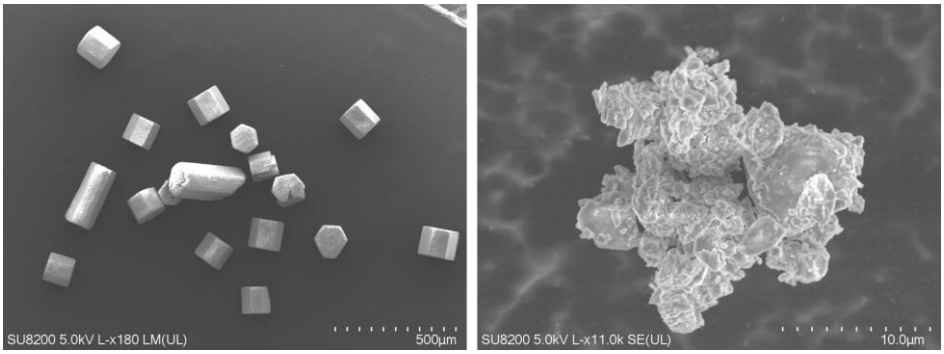

Figure S16. SEM image of the initial Cu-Ni-POM crystals with size of 0.16~0.19 mm, with which the catalytic 3a yield is 79% in 12 hours (left picture); right is the Cu-Ni-POM crystals whose size is 0.5~2.5μm, with that the catalytic 3a yield is 97% in 12 hours (right picture). These results demonstrated the surface area is the crucial factor for high yield.

8. Plausible C-N bond forming reaction mechanism.

Scheme S1. Plausible C-N bond forming reaction mechanism.

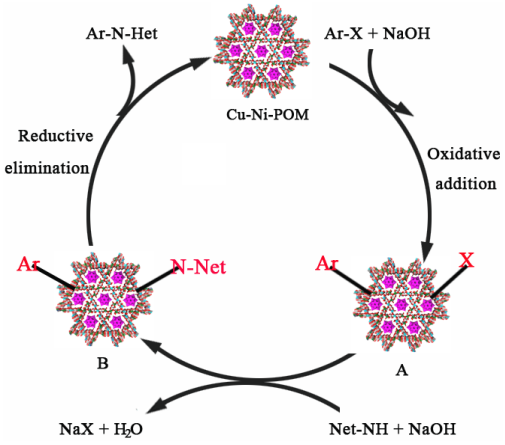

Based on previous literature reports[S2, S6-S8], the reaction mechanism for this transformation is proposed and shown in Scheme S1 that catalysis C-N bond coupling may occur on the exposed copper site (catalyst) and nickel metal/POM (Co-catalyst) concerted catalysis. In the presence of base, oxidative addition of Cu-Ni-POM to aryl halides provided Cu-complex A. And then, the nucleophilic substitution of intermediate A with N-containing heterocycles gave B, followed by reductive elimination led to the desired N-arylated products and regenerated the active copper catalyst.

9. [1]HNMR, GC-MS and GC data of the C-N bond forming Reaction products.

1-phenyl-1*H*-pyrrole

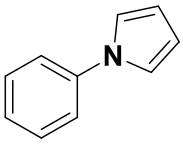

Isolated yield: 93%. ^{1}H NMR (500 MHz, $CDCl_3$) δ 7.46 – 7.37 (m, 4H), 7.25 – 7.23 (m, 1H), 7.10 (d, *J* = 2.0 Hz, 2H), 6.36 (d, *J* = 1.9 Hz, 2H).

GC-MS: m/z = 143 $[M]^+$

GC yield :100%

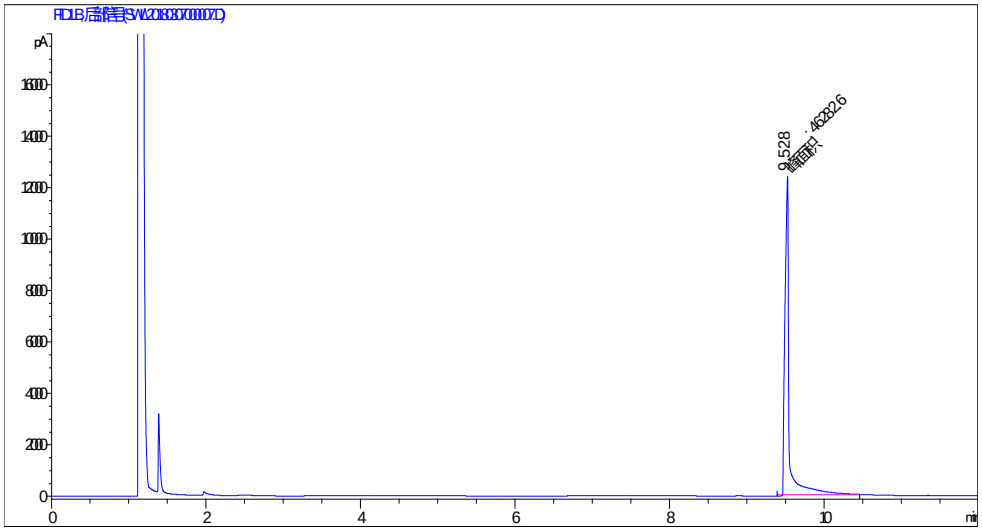

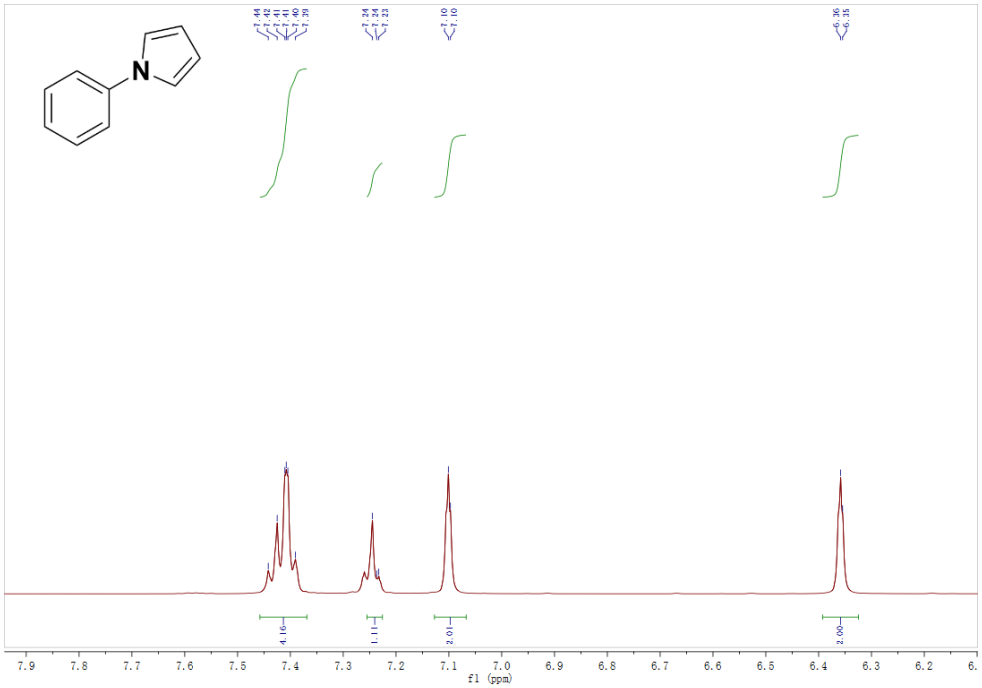

1-(*p*-Tolyl)-1*H*-pyrrole

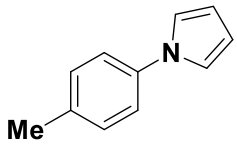

Isolated yield: 97%.^{1}H NMR (500 MHz, $CDCl_3$) δ 7.31 (d, *J* = 8.3 Hz, 2H), 7.24 (d, *J* = 8.0 Hz, 2H), 7.09 (d, *J* = 1.9 Hz, 2H), 6.37 (d, *J* = 1.7 Hz, 2H), 2.40 (s, 3H).

GC-MS: m/z = 157 $[M]^+$

GC Yield: 100%

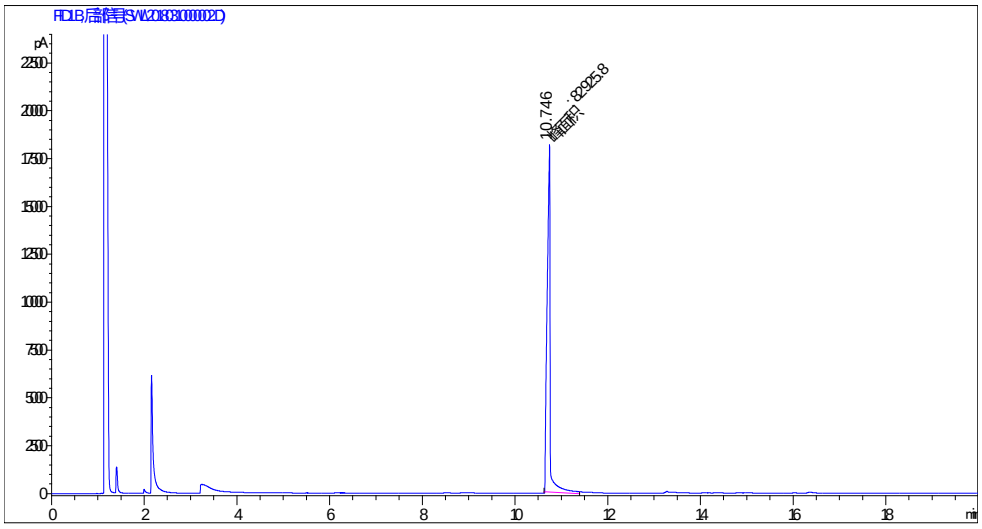

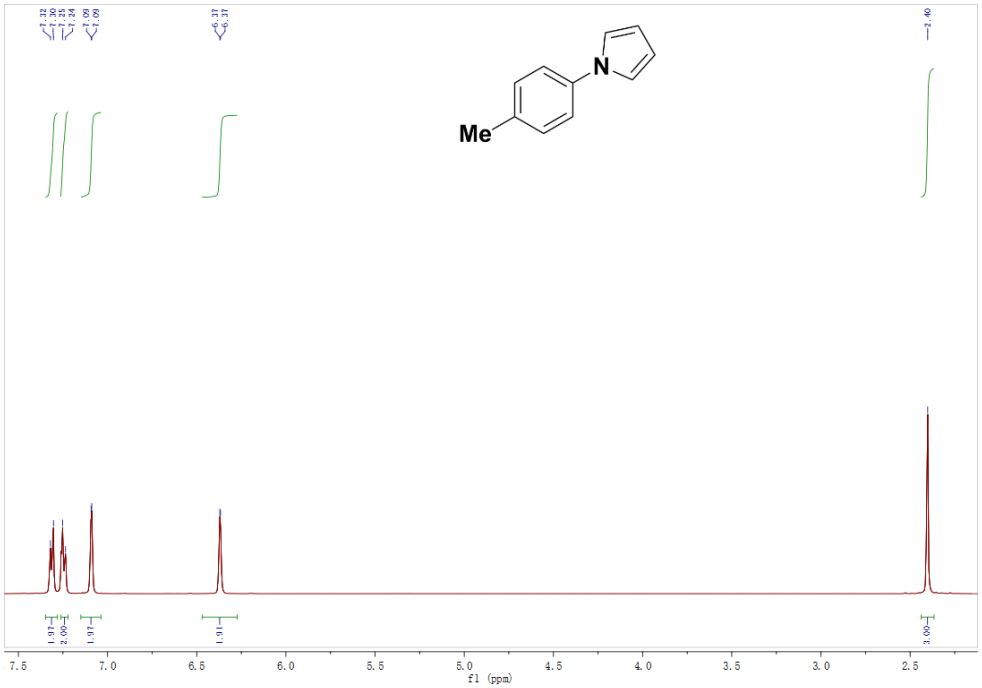

1-([1,1'-Biphenyl]-4-yl)-1*H*-pyrrole.

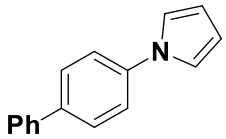

Isolated yield: 98%. ^{1}H NMR (500 MHz, $CDCl_3$) δ 7.70 – 7.58 (m, 4H), 7.47 (t, *J* = 8.0 Hz, 4H), 7.37 (dd, *J* = 10.6, 4.1 Hz, 1H), 7.18 – 7.11 (m, 2H), 6.44 – 6.34 (m, 2H).

GC-MS (m/z): 219 $[M]^+$

GC Yield: 100%

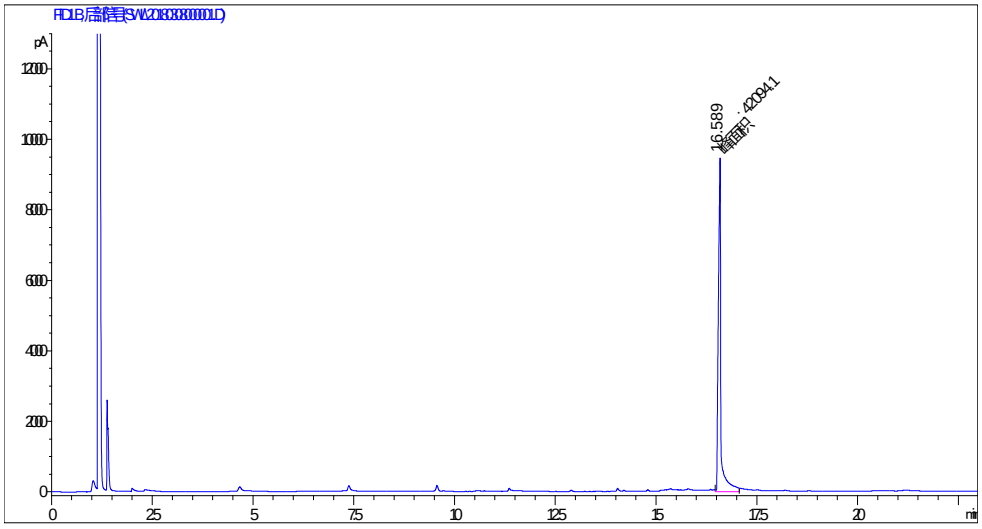

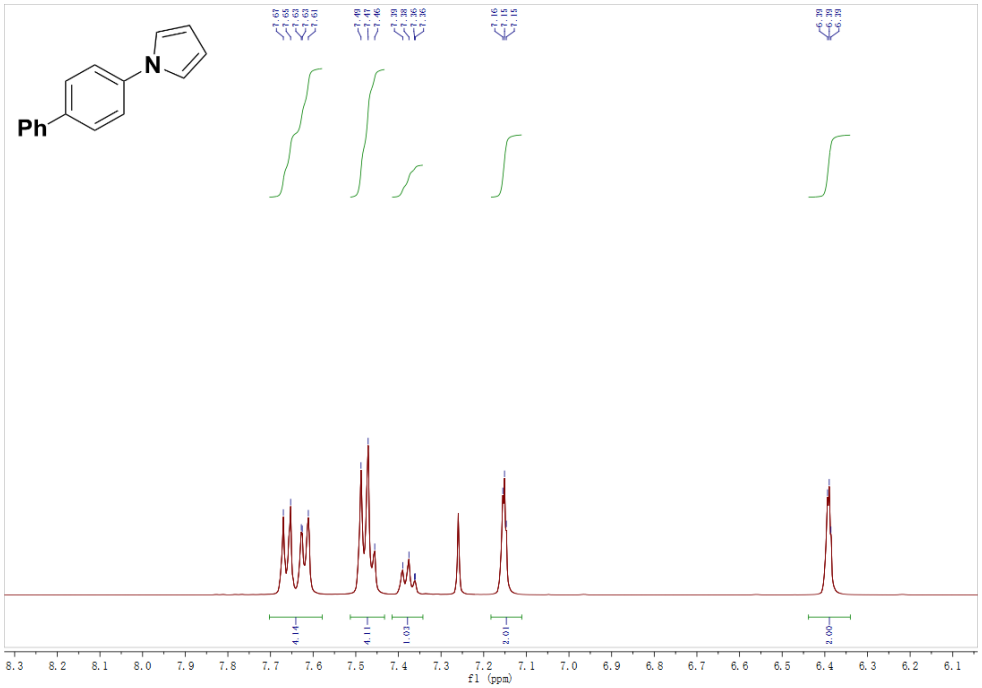

1-(4-Methoxyphenyl)-1*H*-pyrrole

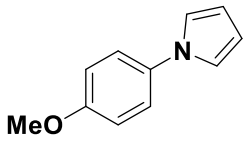

Isolated yield: 90%. ^{1}H NMR (500 MHz, $CDCl_3$) δ 7.32 (d, *J* = 8.9 Hz, 2H), 7.08 – 6.90 (m, 4H), 6.34 (d, *J* = 1.9 Hz, 2H), 3.85 (s, 3H).

GC-MS (m/z):173 $[M]^+$

GC Yield: 100%

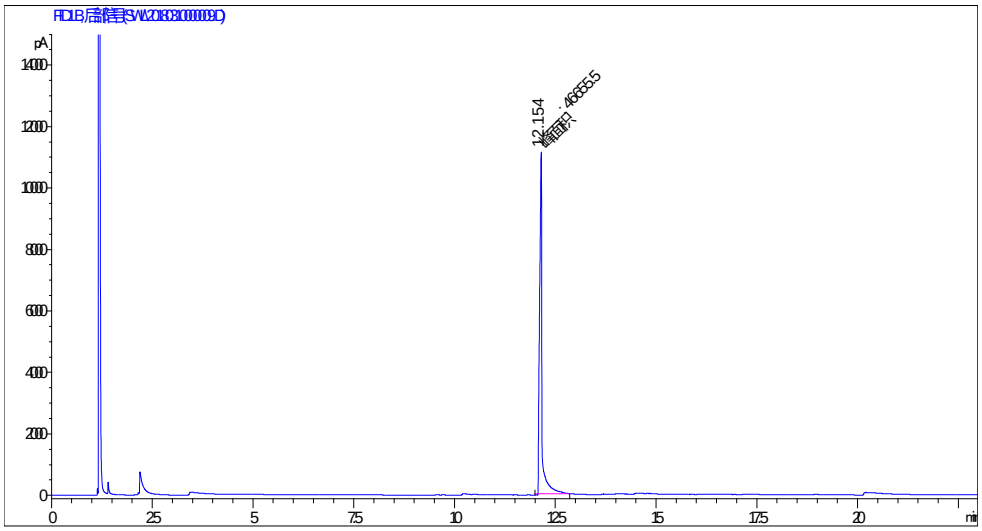

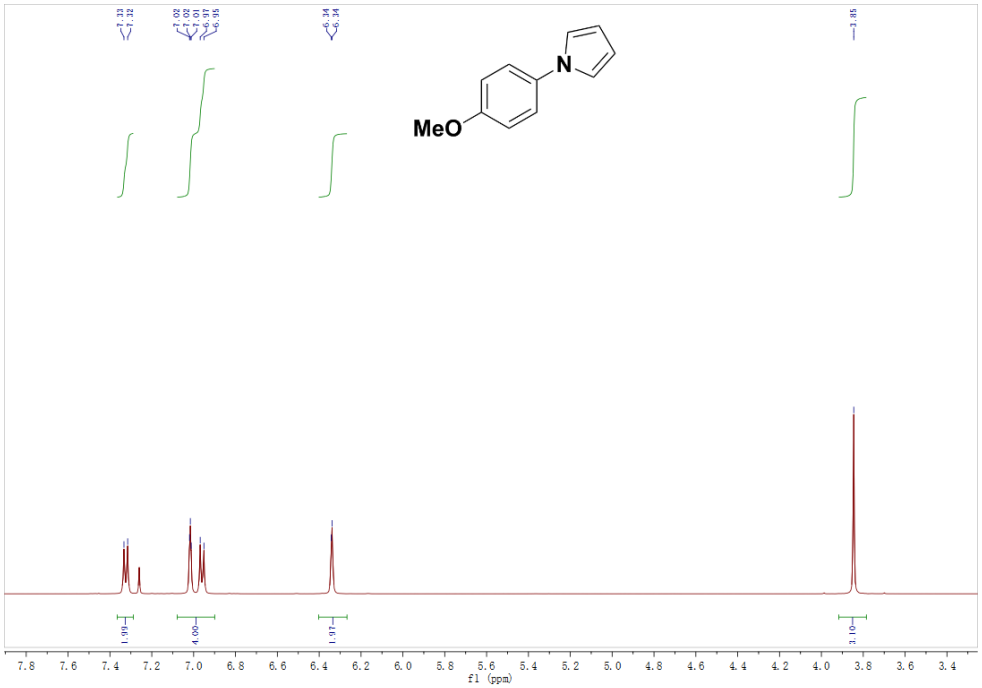

1-(4-Chlorophenyl)-1*H*-pyrrole.

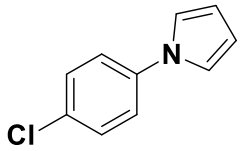

Isolated yield: 88%. ^{1}H NMR (500 MHz, $CDCl_3$) δ 7.40 (d, *J* = 8.8 Hz, 2H), 7.33 (d, *J* = 8.8 Hz, 2H), 7.06 (d, *J* = 1.9 Hz, 2H), 6.38 (d, *J* = 1.9 Hz, 2H).

GC-MS (m/z):177 $[M]^+$

GC Yield: 97%

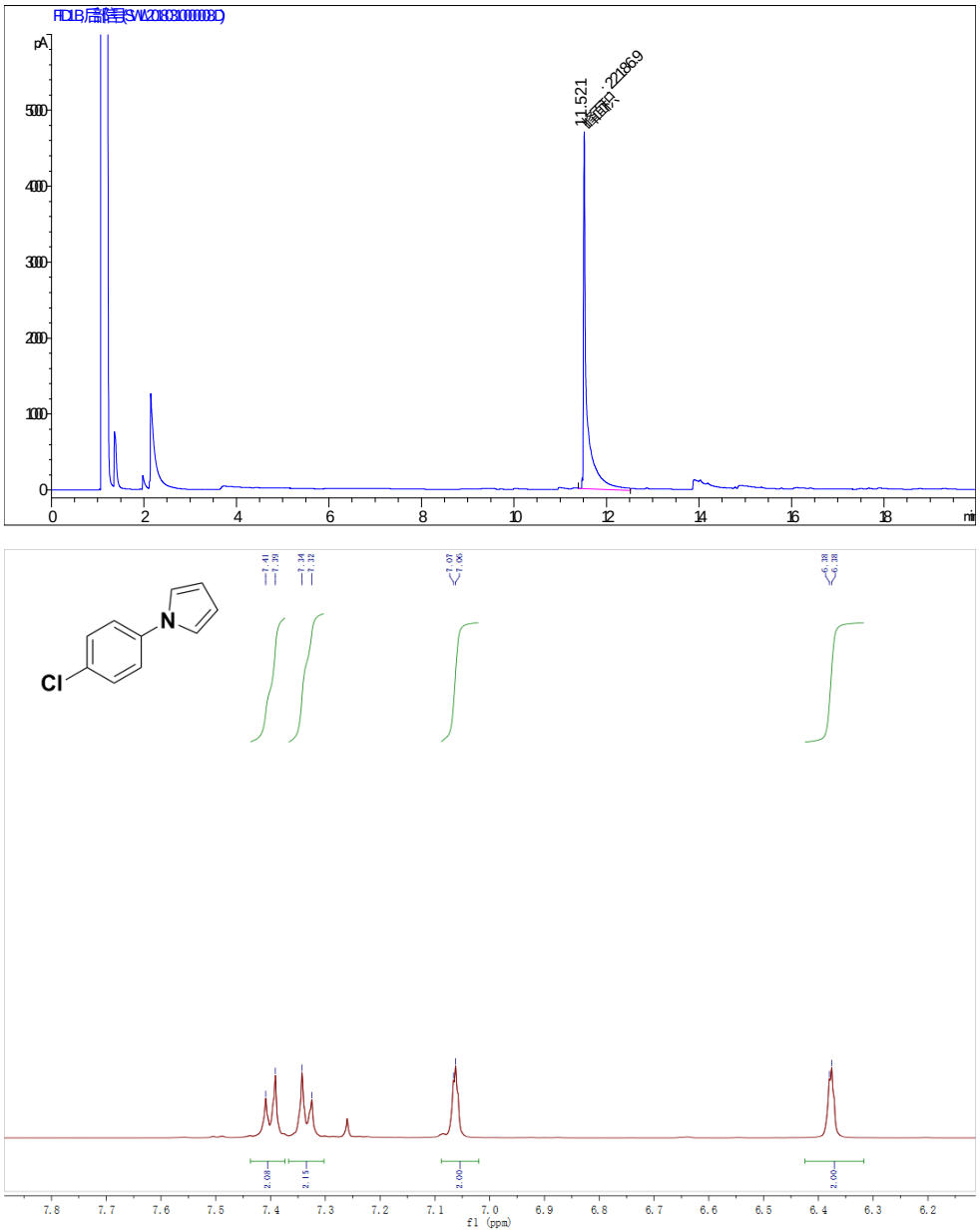

1-phenyl-1*H*-imidazole.

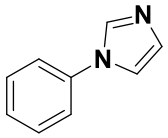

Isolated yield: 91%. ^{1}H NMR (500 MHz, DMSO-d_6) δ 8.27 (s, 1H), 7.76 (s, 1H), 7.65 (d, *J* = 7.7 Hz, 2H), 7.51 (t, *J* = 7.9 Hz, 2H), 7.36 (t, *J* = 7.4 Hz, 1H), 7.12 (s, 1H).

GC-MS (m/z):144 $[M]^{+}$

GC Yield: 96%

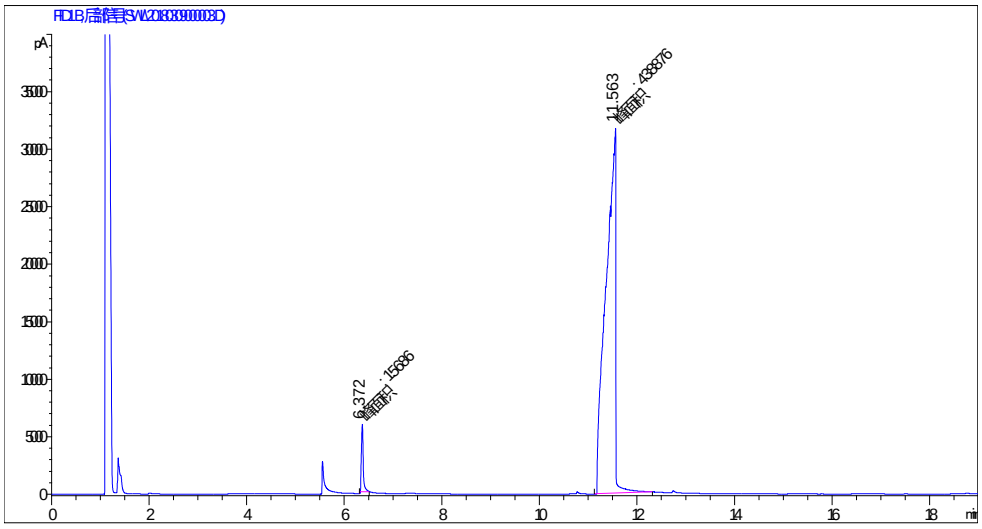

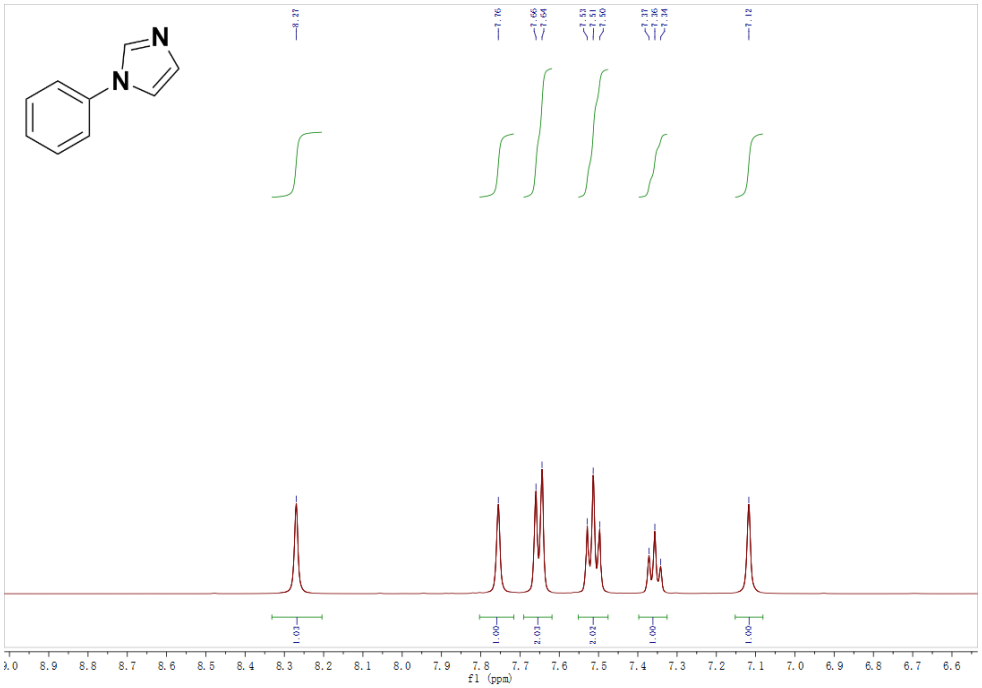

1-(*p*-Tolyl)-1*H*-imidazole.

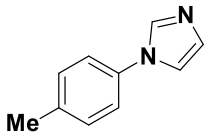

Isolated yield: 93%. ^{1}H NMR (500 MHz, DMSO-d_6) δ 8.20 (s, 1H), 7.70 (s, 1H), 7.52 (d, J = 8.3 Hz, 2H), 7.31 (d, J = 8.1 Hz, 2H), 7.09 (s, 1H), 2.34 (s, 3H).

GC-MS (m/z):158 $[M]^+$

GC Yield: 100%

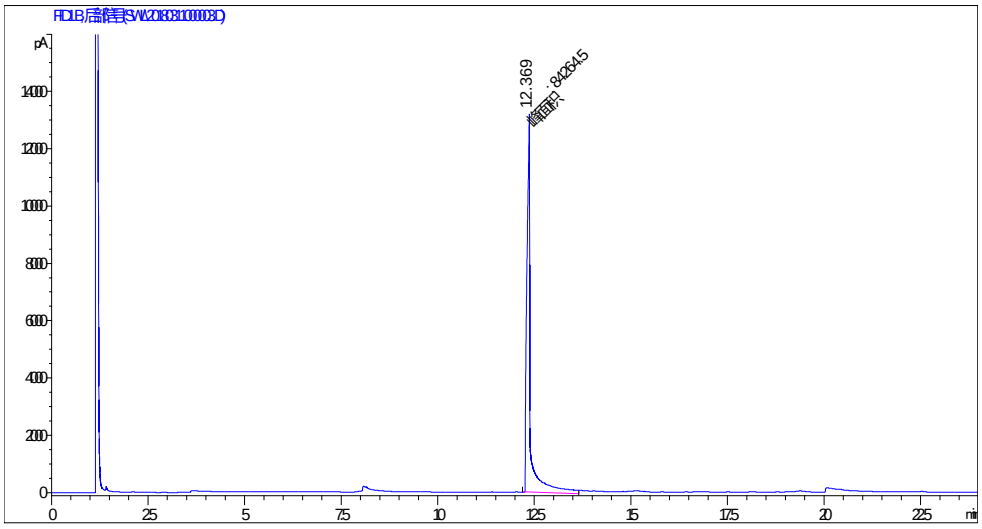

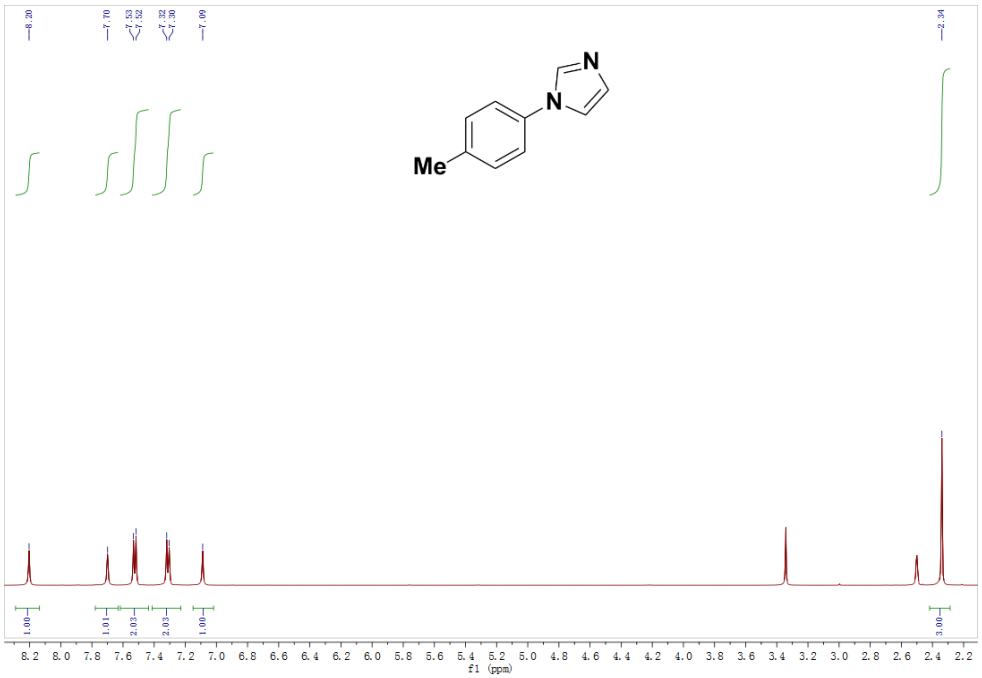

1-([1,1'-biphenyl]-4-yl)-1H-imidazole.

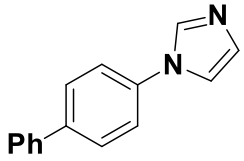

Isolated yield: 93%.^{1}H NMR (500 MHz, DMSO-d_6) δ 8.34 (s, 1H), 7.81 (d, J = 8.2 Hz, 3H), 7.73 (dd, J = 17.5, 7.9 Hz, 4H), 7.48 (t, J = 7.6 Hz, 2H), 7.39 (t, J = 7.3 Hz, 1H), 7.14 (s, 1H).

GC-MS (m/z):220 $[M]^{+}$

GC Yield: 100%

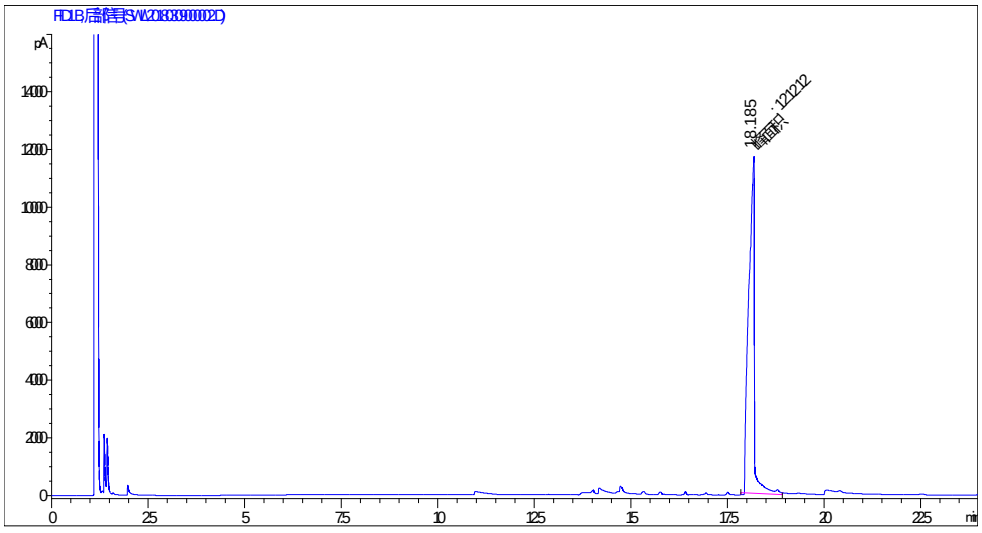

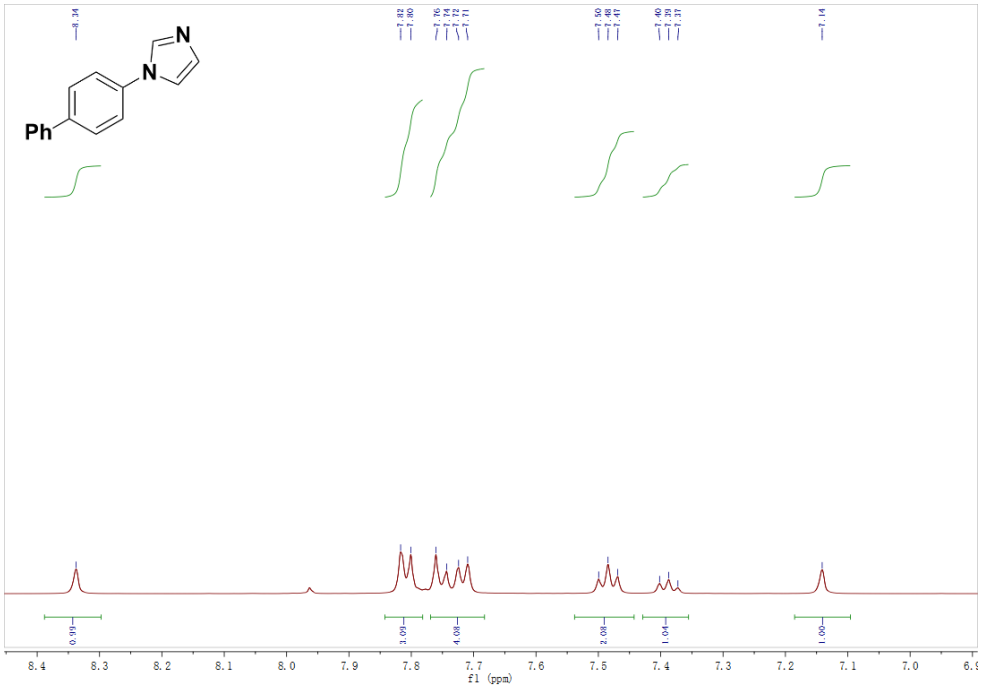

1-(4-Methoxyphenyl)-1*H*-imidazole.

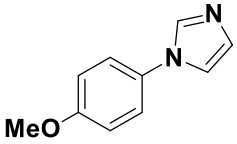

Isolated yield: 87%. ^{1}H NMR (500 MHz, $CDCl_3$) δ 7.76 (d, *J* = 4.9 Hz, 1H), 7.29 (d, *J* = 8.9 Hz, 2H), 7.19 (d, *J* = 10.3 Hz, 2H), 6.98 (d, *J* = 8.9 Hz, 2H), 3.84 (s, 3H).

GC-MS (m/z):174 $[M]^+$

GC Yield: 94%

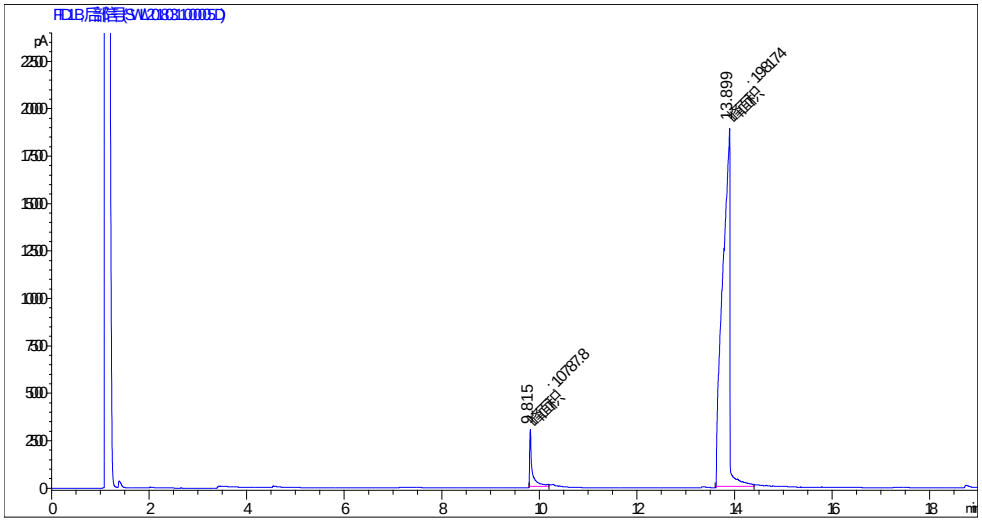

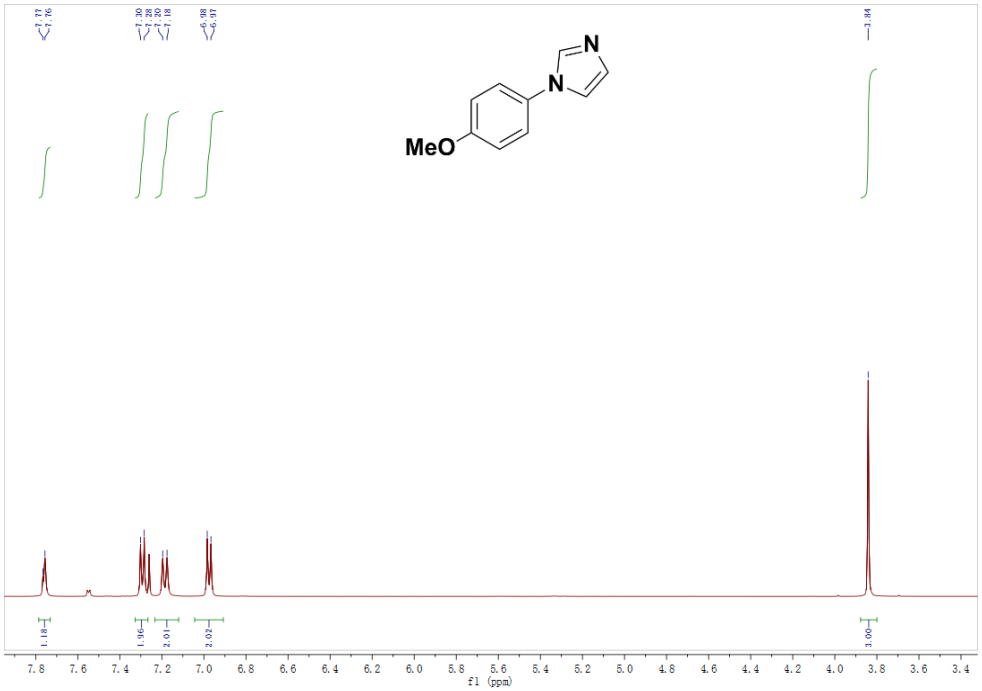

1-(4-Chlorophenyl)-1*H*-imidazole.

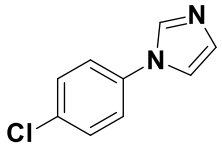

Isolated yield: 85%. ^{1}H NMR (500 MHz, $CDCl_3$) δ 7.84 (s, 1H), 7.46 (d, *J* = 8.7 Hz, 2H), 7.34 (d, *J* = 8.7 Hz, 2H), 7.27 (s, 1H), 7.22 (s, 1H).

GC-MS (m/z):178 $[M]^+$

GC Yield: 96%

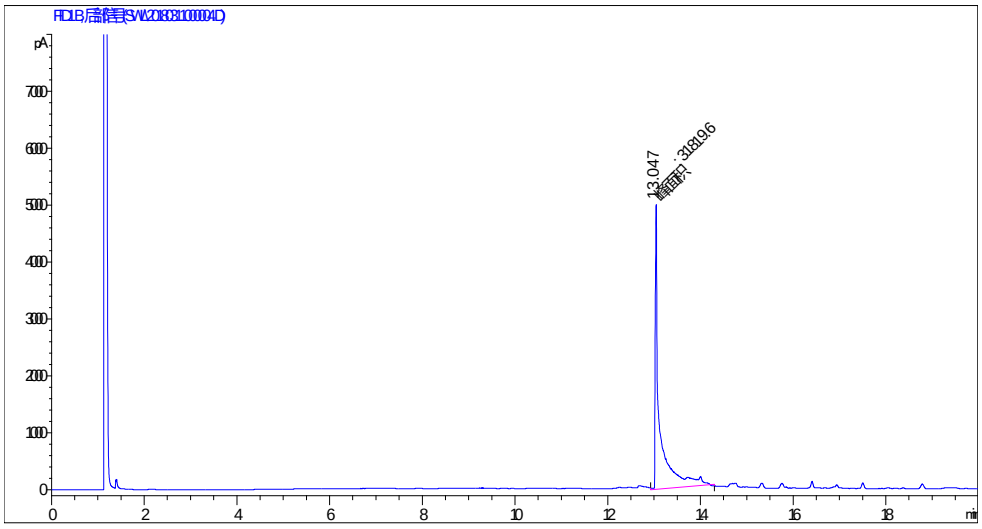

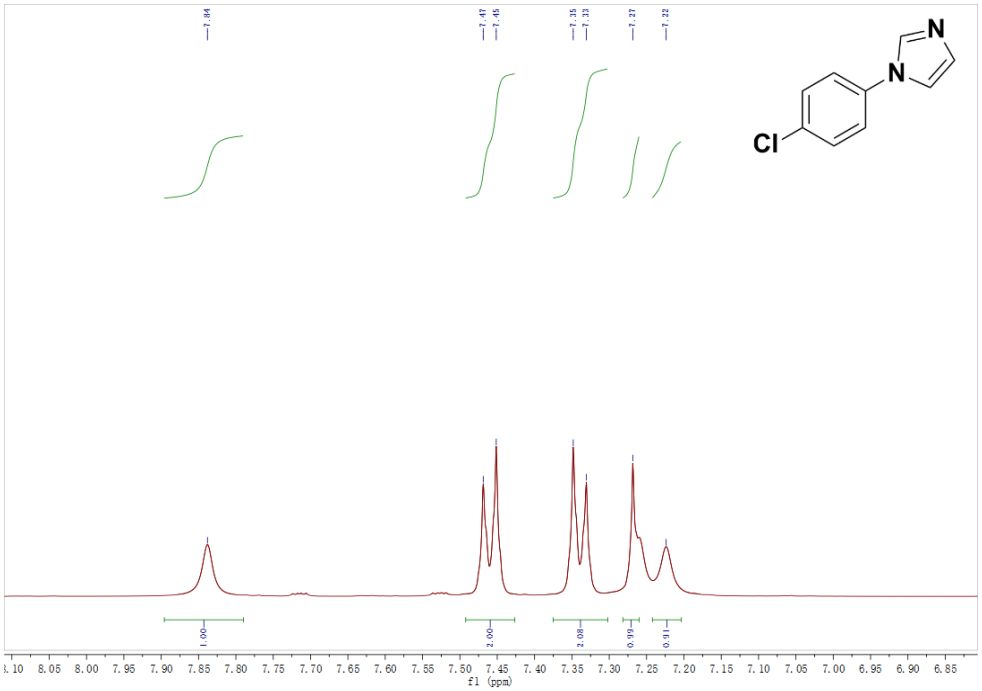

1-phenyl-1*H*-1,2,4-triazole.

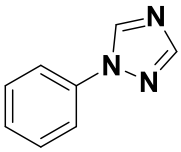

Isolated yield: 61%. ^{1}H NMR (500 MHz, $CDCl_3$) δ 8.57 (s, 1H), 8.11 (s, 1H), 7.68 (d, *J* = 7.7 Hz, 2H), 7.51 (t, *J* = 7.9 Hz, 2H), 7.40 (t, *J* = 7.4 Hz, 1H).

GC-MS (m/z):145 $[M]^+$

GC Yield: 65%

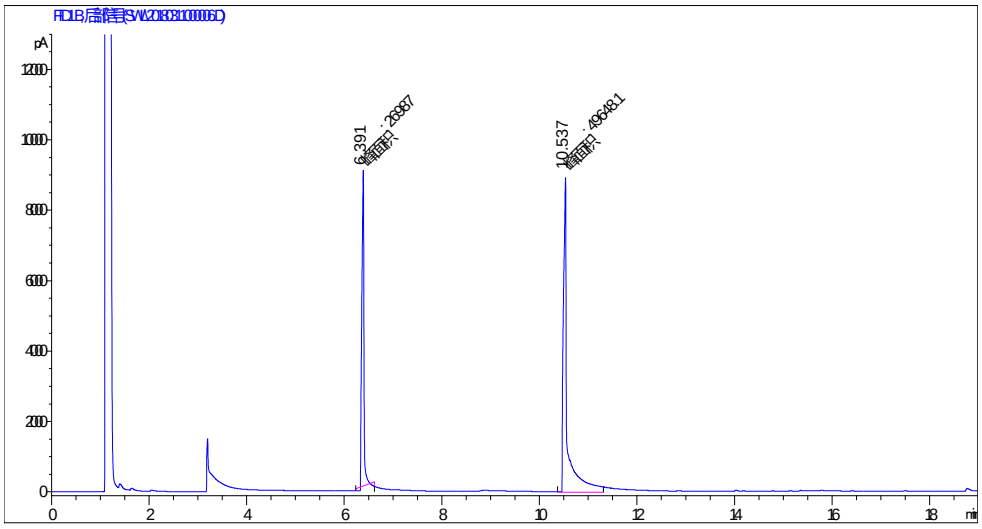

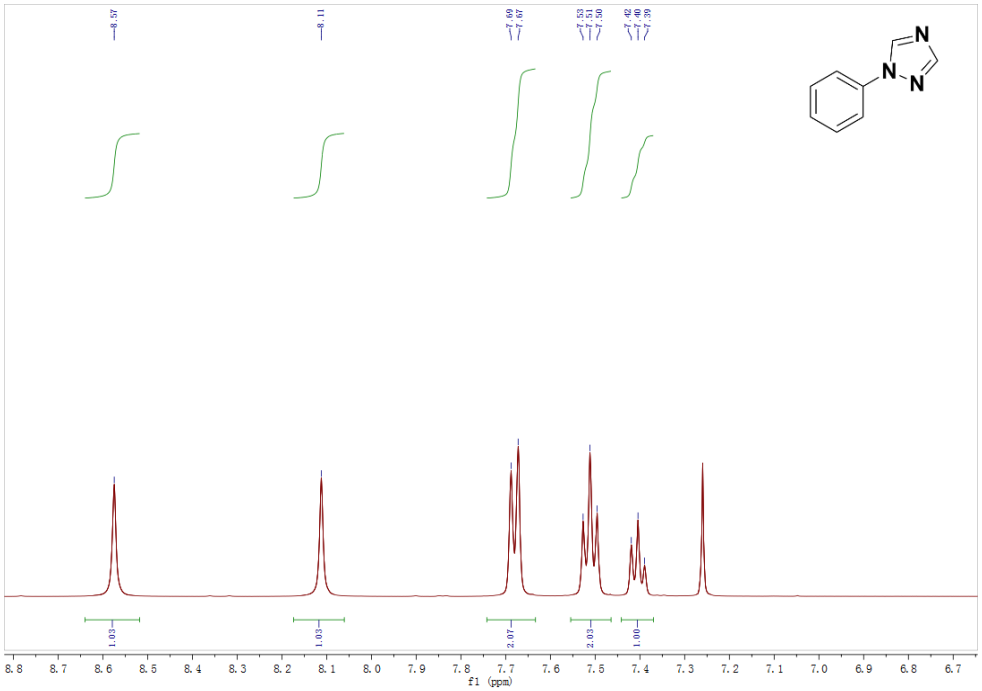

1-(4-Chlorophenyl)-1*H*-1,2,4-triazole.

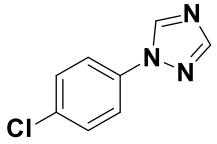

Isolated yield: 35%. ^{1}H NMR (500 MHz, $CDCl_3$) δ: 8.55 (s, 1H), 8.10 (s, 1H), 7.62-7.64 (m, 2H), 7.47-7.49 (m, 2H).

GC-MS (m/z):179 $[M]^+$

GC Yield: 37%

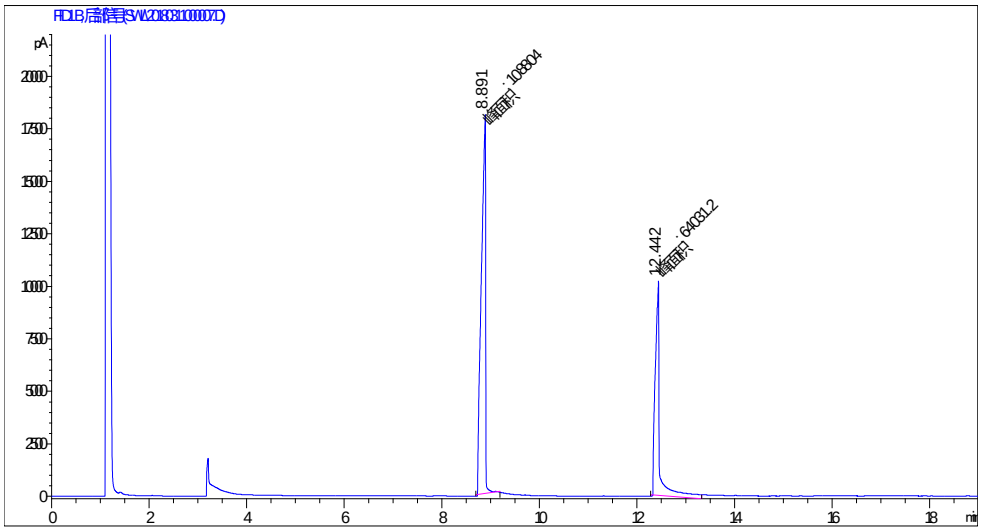

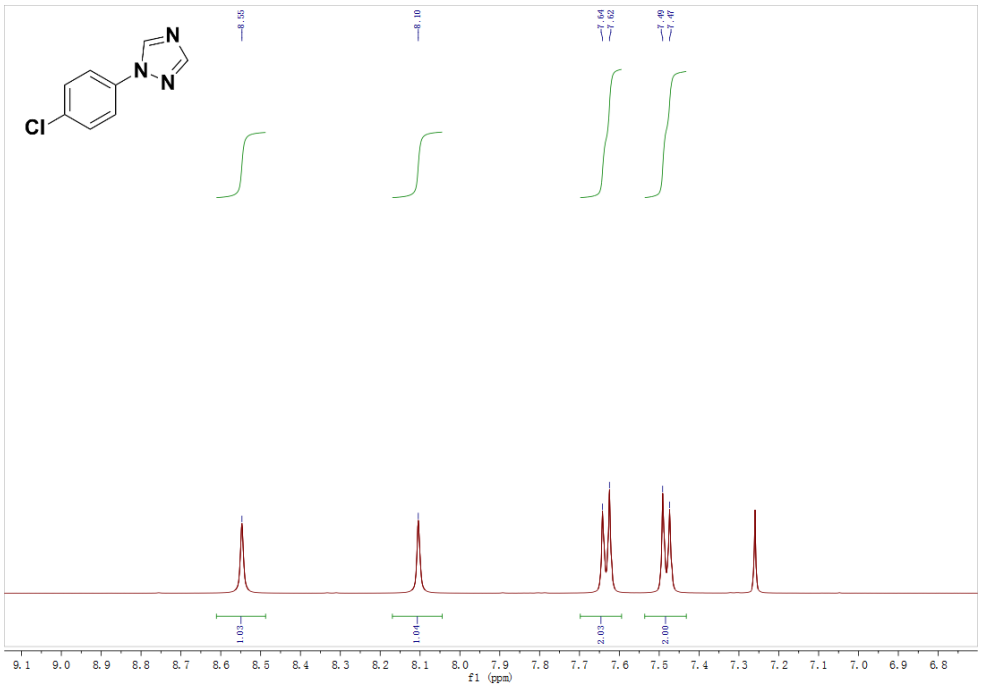

10. References

S1 Z. G. Gu, S. Grosjean, S. Bräse, C. Wöll and L. Heinke, *Chem. Commun.*, 2015, **51**, 8998.

S2 Z. H. Li, F. Meng, J. Zhang, J. W. Xie and B. Dai, *Org. Biomol. Chem.*, 2016, **14**, 10861.

S3 SMART, Data collection software (version 5.629) (Bruker AXS Inc., Madison, WI, 2003).

S4 SAINT, Data reduction software (version 6.45) (Bruker AXS Inc., Madison, WI, 2003).

S5 Sheldrick, G. M. SHELXTL97, Program for crystal structure solution (University of Göttingen: Göttingen, Germany, 1997)

S6 M. Gopiraman, S. G. Babu, Z. Khatri, W. Kai, Y. A. Kim, M. Endo, R. Karvembu and I. S. Kim, *Carbon*, 2013, **62**, 135.

S7 T. Truong, C. V. Nguyen, N. T. Truong and N. T. S. Phan, *RSC Adv*., 2015, **5**, 107547.

S8 S. Jammi, S. Sakthivel, L. Rout, T. Mukherjee, S. Mandal, R. Mitra, P. Saha and T. Punniyamurthy, *J. Org. Chem.*, 2009, **74**, 1971.